The seven-triangle longest-side partition of triangles and mesh quality improvement

Alberto Márquez[a], Auxiliadora Moreno-González[a,*], Ángel Plaza[b], José P. Suárez[c]

[a]Department of Applied Mathematics I, University of Seville, Spain
[b]Department of Mathematics, University of Las Palmas de Gran Canaria, Spain
[c]Department of Cartography and Graphic Engineering, University of Las Palmas de Gran Canaria, Spain

Keywords:

Refinement
Longest-edge based algorithms
Improvement of mesh quality

A B S T R A C T

A new triangle partition, the seven-triangle longest-edge partition, based on the trisection of the edges is presented and the associated mesh quality improvement property, discussed. The seven-triangle longest-edge (7T-LE) partition of a triangle t is obtained by putting two equally spaced points per edge. After cutting off three triangles at the corners, the remaining hexagon is subdivided further by joining each point of the longest-edge of t to the base points of the opposite sub-triangle. Finally, the interior quadrangle is subdivided into two sub-triangles by the shortest diagonal. The self-improvement property of the 7T-LE partition is discussed, delimited and compared to the parallel property of the four-triangle longest-edge (4T-LE) partition. Global refinement strategies, combining longest-edge with self-similar partitions, are proposed, based on the theoretical geometrical properties.

1. Introduction

In the context of finite element methodology, the adaptability of the mesh and the analysis of the approximation error are important issues to be addressed [1]. In recent years, many partitions and associated refinement and coarsening algorithms have been proposed and studied [2–7]. In the area of adaptive finite element methods, mesh refinement algorithms that maintain the *non-degeneracy* of the elements and the *conformity* and *smoothness* of the grid are certainly desirable. Non-degeneracy means that the minimum angle of the triangles is bounded away from zero when the partition or refinement is applied. Conformity refers to the requirement that the intersection of non-disjoint triangles is either a common vertex or a common edge. The smoothness condition states that the transition between small and large elements should be gradual.

Non-degeneracy, conformity and smoothness are also desirable properties in adaptive tessellation of NURBS surfaces [8]. In this sense, Delaunay meshes have been widely used, since they avoid long, `skinny' triangles and produce the maximum possible smallest-internal angle of any triangle [9]. Refinement techniques are also used for enhancement of mesh obtained from trimmed NURBS surfaces. See an application of this in [10]. The number of triangles can be further increased/decreased depending on the application requirements.

Longest-edge based algorithms have been used with Delaunay triangulation for the quality triangulation problem [11,12], with details of the fractal properties of the meshes obtained by these algorithms also given [5,13,14].

Some refinement methods have had exact angle counts since they first existed [2,3,6,15] and, consequently, the non-degeneracy of the triangulation is proved. The four-triangle longest-edge (4T-LE) refinement algorithm proposed by Rivara [16], given that it is based on the longest-edge bisection, never produces an angle smaller than half the minimum original angle [16,17], whilst, moreover, revealing remarkable mesh quality improvement between certain limits, as recently studied in [18]. However, this mesh quality improvement depends on the geometry of the initial triangle as will be underlined herein.

In search of a better mesh quality improvement by iterative partition of the mesh, in this paper, we have introduced a new triangle partition, the seven-triangle longest-edge (7T-LE) partition. This partition, first, positions two equally spaced points per edge and, then, the interior of the triangle is divided into seven sub-triangles in a manner compatible with the subdivision of the edges. Three of the new sub-triangles are similar to the original, two are similar to the new triangle also generated by the 4T-LE, and the other two triangles are, in general, better shaped. We compare the evolution of a standard quality measurement for the iterative application of the 7T-LE partition to an initial triangle, first with a Delaunay-type partition, and then using the 4T-LE partition.

The paper is organized as follows: the 4T-LE partition and the self-improvement property achieved via its application is summarized in Section 2. We go on to present the 7T-LE partition in Section 3,

* Corresponding author. Tel.: +34 954486482; fax: +34 954488160.
E-mail addresses: almar@us.es (A. Márquez), auxiliadora@us.es (A. Moreno-González), aplaza@dmat.ulpgc.es (Á. Plaza), jsuarez@dcegi.ulpgc.es (J.P. Suárez).

with some of its proven properties. Section 3 ends by comparing different strategies for partitioning a single triangle by combining longest-edge based partitions with self-similar partitions. Numerical experiments are provided in Section 4 proving that the new 7T-LE partition is comparatively better than the 4T-LE partition, and is also advantageous in many scenarios with respect to a 7-triangle local Delaunay-based partition.

2. Longest-edge triangular partitions

Here the 4T-LE partition and its self-improvement is summarized. The section closes with an example illustrating the limits of the characteristics of improvement.

In the following, for any triangle t, the edges and angles will be, respectively, denoted in decreasing order $r_1 \geqslant r_2 \geqslant r_3$ and $\gamma \geqslant \beta \geqslant \alpha$. Furthermore, $t(\alpha, \beta, \gamma)$ will be the class of similar triangles with angles $\gamma \geqslant \beta \geqslant \alpha$. Interchangeably, t will represent an element of the class $t \in t(\alpha, \beta, \gamma)$ or the class itself.

Definition 1. The longest-edge (LE) partition of a triangle t_0 is obtained by joining the midpoint of the longest edge of t_0 with the opposite vertex (Fig. 1(a)). The 4-triangle longest-edge (4T-LE) partition is obtained by joining the midpoint of the longest edge to the opposite vertex and to the midpoints of the two remaining edges (see Fig. 1(b)).

It should be noted here that in order to ensure the conformity over the mesh when local refinement based on the 4T-LE partition is used, two additional three-triangle (3T) partitions are applied along with the longest-edge (LE) partition [16]. The 3T partition of a triangle t is obtained by performing, first, the LE partition of t, and then, one of the two sub-triangles generated is further bisected by joining the midpoint of the longest-edge of t with the midpoint of the opposite edge. Fig. 2 shows these 3T partitions. The 3T partition of a triangle t in which the second longest-edge of t is also subdivided will be denoted here 3T-LE.

Since the first 4T-LE partition of any triangle t_0 introduces two new edges parallel to the edges of t_0, the same first 4T-LE partition of a single triangle t_0 produces two triangles similar to t_0, and two (potentially) new similar triangles t_1; and, consequently, the iterative 4T-LE partition of any triangle t_0 introduces (at most) one new dissimilar triangle per iteration [19]. See Fig. 3, in which two different situations for the 4T-LE partition are presented. On the left of the figure, the 4T-LE partition of triangle t_1 produces a new triangle t_2. On the right, however, the generation of new triangles stops at the second stage of refinement.

The iterative 4T-LE partition produces a finite sequence of `better' triangles satisfying the properties illustrated in the following diagram until triangle t_N becomes non-obtuse [19]:

$$\begin{array}{ccccccc} t_0 & \rightarrow & t_1 & \rightarrow & t_2 & \rightarrow \ldots \rightarrow & t_N \\ \text{(obtuse)} & & \text{(obtuse)} & & \text{(obtuse)} & & \text{(non-obtuse)} \\ \alpha_0 & & \alpha_1 > \alpha_0 & & \alpha_2 > \alpha_1 & & \alpha_N > \alpha_{N-1} \\ \gamma_0 & & \gamma_1 \leqslant \gamma_0 - \alpha_1 & & \gamma_2 \leqslant \gamma_1 - \alpha_2 & & \gamma_N \leqslant \gamma_{N-1} - \alpha_N \end{array}$$

Diagram 1. (From [19])

where α_i and γ_i are, respectively, the smallest and the largest angles of triangle t_i. The arrow emanating from triangle t_i to triangle t_{i+1} means that the (first) 4T-LE partition of triangle t_i produces the new dissimilar triangle t_{i+1}.

2.1. Mesh quality improvement for the 4T-LE partition

We refer the reader to [18] in which the self-improvement property of the 4T-LE partition has been studied in detail. The bounds of the minimum and second largest angles, when the 4T-LE partition is applied to an initial (obtuse) triangle, are detailed in [18]. By way of example, consider the initial triangle t_0 with angles $(\alpha, \beta, \gamma) = (1.95, 32.595, 145.455)$. The evolution of the smallest angle and largest angle for each of the new triangles generated by the 4T-LE partition is shown in Fig. 4. Therefore, the self-improvement property of the 4T-LE partition, as proven both experimentally and

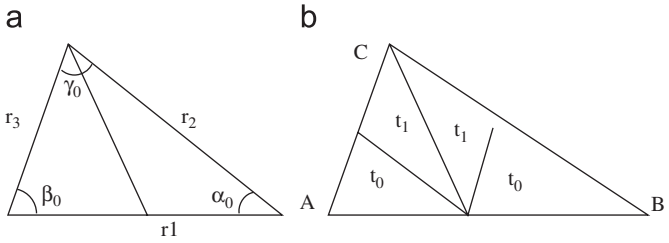

Fig. 1. (a) LE partition of triangle t_0, (b) 4T-LE partition of triangle t_0.

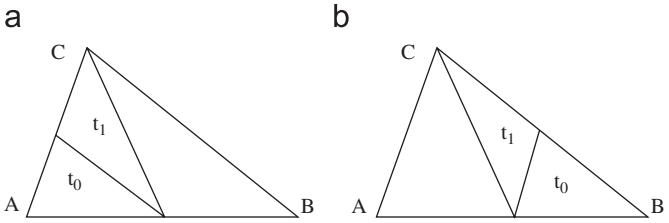

Fig. 2. Three-triangle partitions of triangle t_0 used in local refinement for assuring conformity. 3T-LE of t_0 at the right.

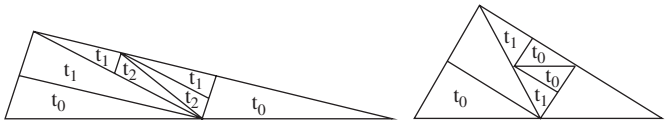

Fig. 3. Two different situations. On the right, the generation of new triangles stops at the second stage of refinement.

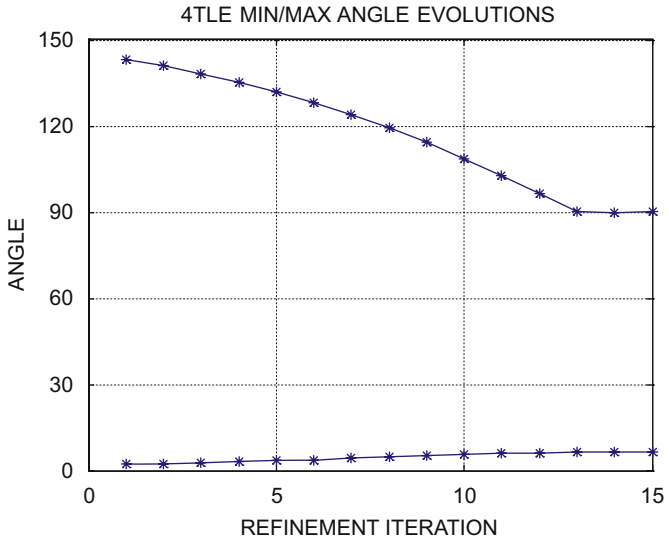

Fig. 4. Evolution of minimum and maximum angles of the new dissimilar triangles generated by the 4T-LE partition, one at a time.

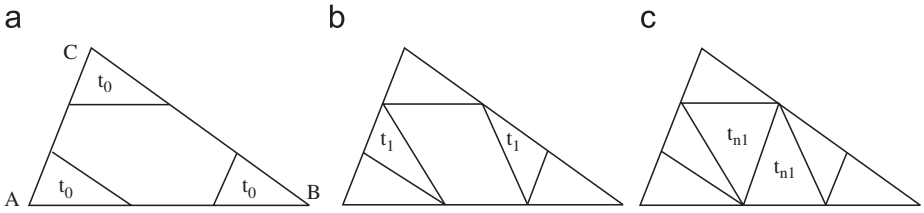

Fig. 5. The 7T-LE partition of triangle $t_0 = \Delta ABC$.

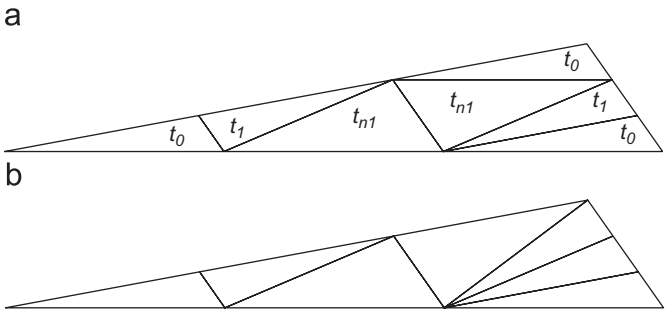

Fig. 6. Two different 7T partitions of an obtuse triangle t_0. (a) 7T-LE partition of t_0. (b) 7T-D partition of t_0.

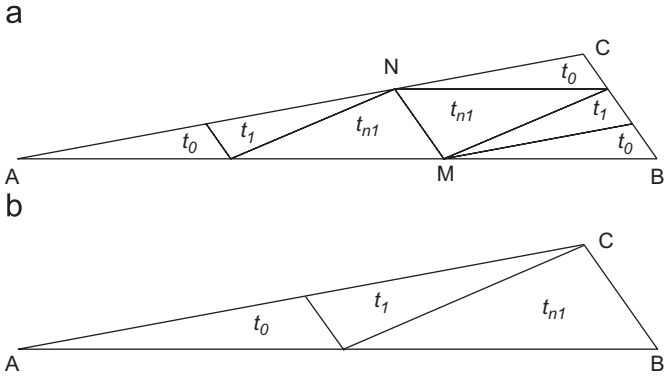

Fig. 7. The 7T-LE partition and 3T-LE partition of an obtuse triangle $t_0 = \Delta ABC$.

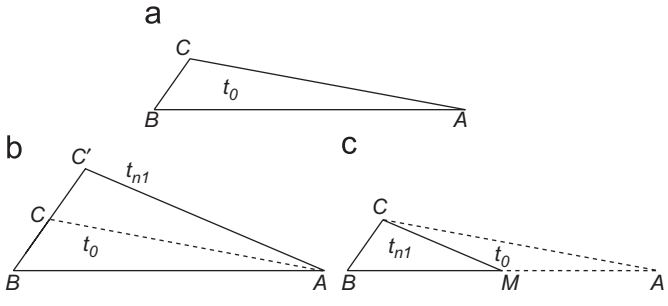

Fig. 8. Two different ways of obtaining new triangles t_{n1}, from triangle t_0. (b) By doubling the shortest edge of t_0. (c) By LE bisection of t_0. t_{n1} is the sub-triangle with acute angle at M.

mathematically in [18], needs to be handled with caution, as the example clearly demonstrates.

Given that the 4T-LE partition is based on the bisection of the edges, by locating midpoints on the edges of the triangle, we have introduced here a new triangular partition based on the trisection of the edges at equally spaced points. Our goal is to study the evolution of the shape of the triangles when this partition is iteratively applied, and to compare it with the behaviour given with the 4T-LE.

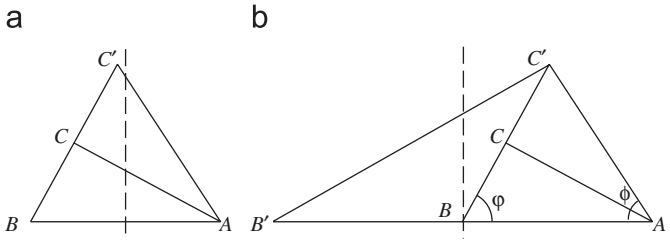

Fig. 9. (a) $|AB| < |BC'| < |AC'|$ and (b) $\phi < \varphi$.

3. The 7T-LE partition

In this section, a new longest-edge partition is presented. This partition is based on the trisection of the edges of the triangle, instead of the bisection of the edges as the 4T-LE.

Definition 2. The 7-triangle longest-edge (7T-LE) partition of a triangle t_0 is obtained as follows:

1. Position two equally spaced points per edge and join them, using parallel segments, to the edges, at the points closest to each vertex (see Fig. 5(a)).
2. Join the two interior points of the longest edge of the initial triangle to the base points of the opposite sub-triangle in such a way that they do not intersect (see Fig. 5(b)).
3. Triangulate the interior quadrangle by the shortest diagonal (see Fig. 5(c)).

It should be noted that, due to parallelism, the first three sub-triangles obtained are similar to the initial one (t_0), whereas the second two sub-triangles are similar to the first-class Rivara triangle (t_1). In general, triangle t_1 is better shaped than triangle t_0. This improvement has already been studied in [18] to which the reader is referred. Finally, the last two triangles are not given with the 4T-LE Rivara partition and, consequently, will be called here, t_{n1}. Note also that the area of sub-triangles t_0 and t_1 is $\frac{1}{9}$ of the area of the initial triangle, whereas the area of each sub-triangle t_{n1} is $\frac{2}{9}$ of the area of the initial triangle.

Basing our hypotheses on the trisection of the edges, some other partitions may be considered. We present here one of these possibilities, also based on a local Delaunay triangulation:

Definition 3. The 7-triangle Delaunay (7T-D) partition of a triangle t_0 is obtained as follows:

1. Position two equally spaced points per edge.

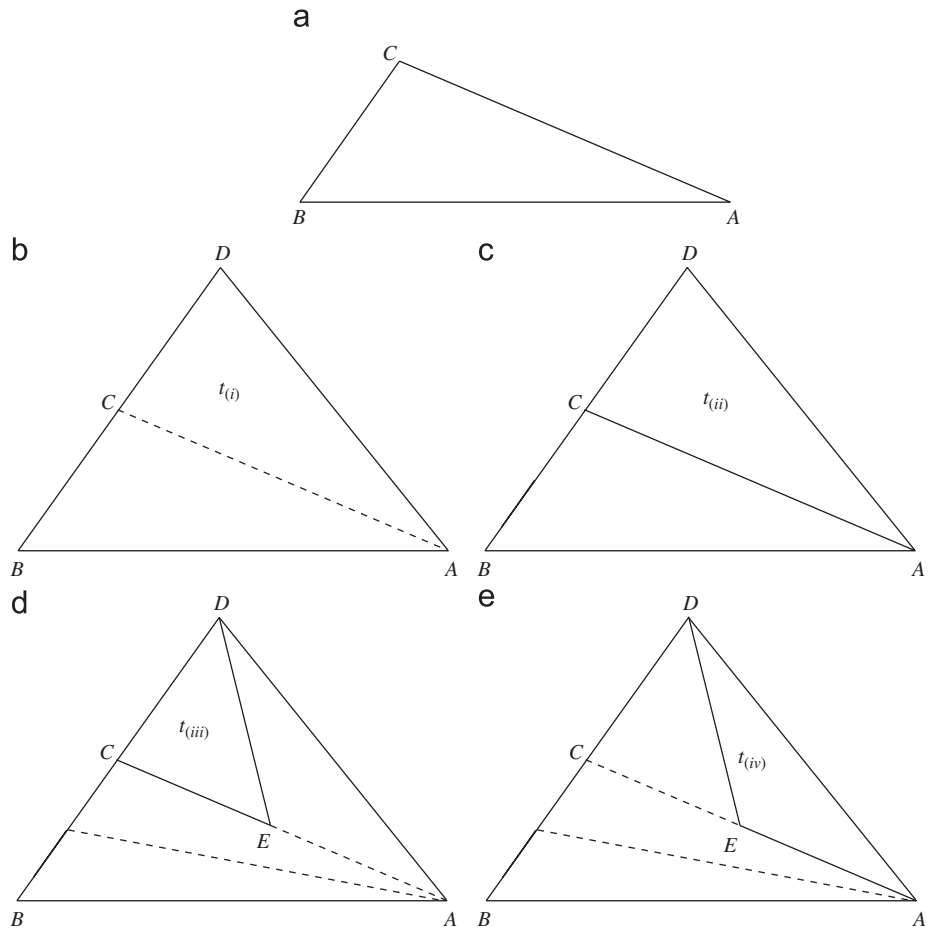

Fig. 10. Sequence of dissimilar t_{n1} triangles generated by the 7T-LE partition: (a) by doubling the shortest edge, (b) triangle $\Delta ABD = t_{(i)}$ is the first one with edge AD not been the shortest edge. (c)–(e) show the following non-similar triangles $t_{(ii)}$, $t_{(ii)}$ and $t_{(iv)}$, for the case in which BD is the longest edge of triangle $\Delta ABD = t_{(i)}$.

2. Triangulate the cloud of points using the Delaunay triangulation (see Fig. 6(b)).

It should be noted that the 7T-D partition is not equivalent to the 7T-LE partition since the division of the interior hexagon depends upon the specific distribution of the distances between the vertices. See Fig. 6.

3.1. Mesh quality improvement for the 7T-LE partition

Before studying in detail the self-improvement property of the 7T-LE partition, note that the new triangle t_{n1} generated by the 7T-LE partition may also be seen as one of the triangles generated by the 3T-LE partition division, used in the local refinement associated with the 4T-LE partition. See Fig. 7 in which triangle t_0, with vertices A, B, and C, is divided by the 7T-LE, and the extreme points of the diagonal of the interior quadrilateral are denoted by M, and N. Notice that, by parallelism, triangle AMN is similar to triangle ABC, and, therefore, the 7T-LE partition of triangle t_0 induces the 3T-LE partition of triangle AMN.

Lemma 4. *The number of dissimilar triangles arising in the iterative application of the 7T-LE partition to any initial triangle $t_0 \equiv \Delta ABC$ is bounded.*

Proof. The 7T-LE partition of a triangle produces two new dissimilar classes of triangles per iteration. One of them is similar to the new triangle generated by the 4T-LE partition. This triangle is noted by t_1 in Fig. 7(a). The other new dissimilar triangle is denoted by t_{n1} in Fig. 7(a). Notice that triangles t_1 and t_{n1} appear also as a result

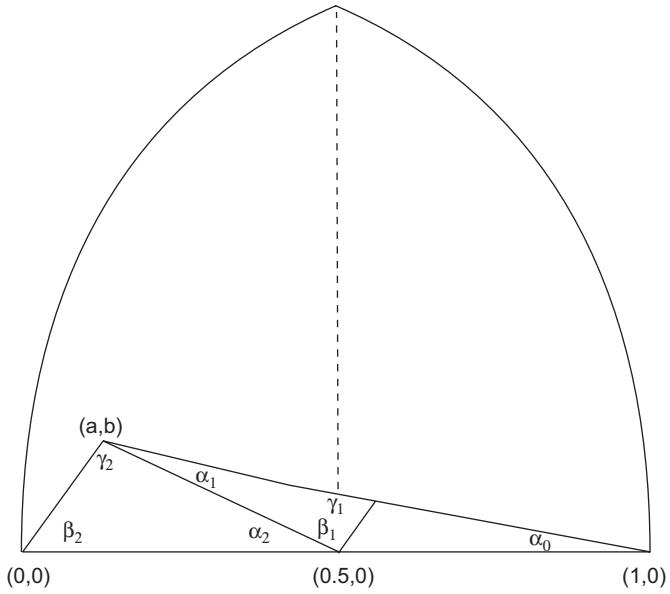

Fig. 11. 3T-LE partition of a random triangle.

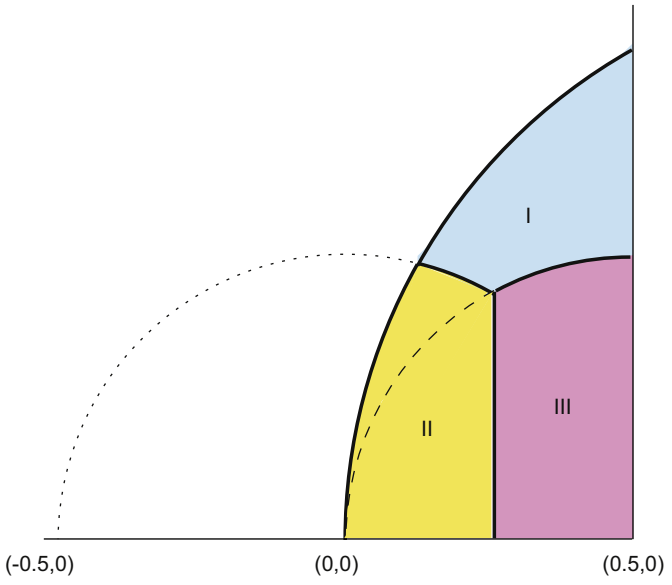

Fig. 12. The smallest angle of t_{n_1} is γ_2 in region *I*, α_2 in region *II* and β_2 in region *III*.

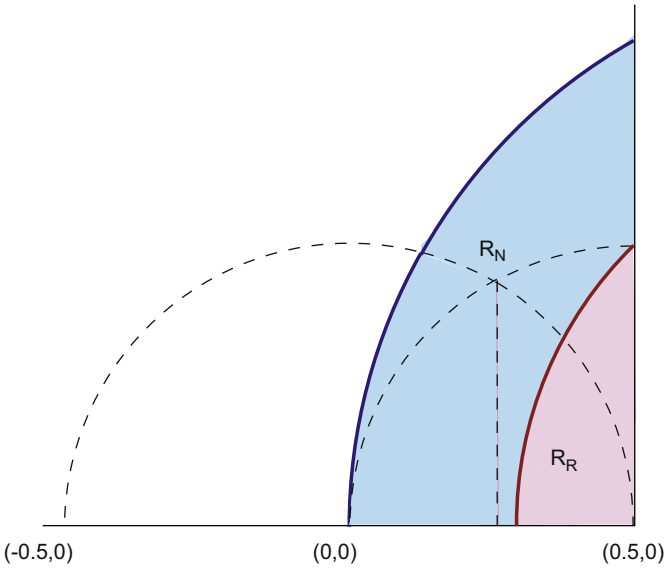

Fig. 13. Regions R_R and R_N.

of the 3T-LE partition of the initial triangle, see Fig. 7(b). Since the number of dissimilar triangles arising in the iterative application of the 4T-LE partition to any triangle t_0 is bounded [18,19], it is enough, here, to prove that the number of dissimilar triangles different from those generated by the 4T-LE partition, is also bounded.

Let us presume that the edges of $t_0 \equiv \Delta ABC$ verify that $|BC| < |AC| < |AB|$. The way to obtain a triangle similar to t_{n1}, is to double the shortest edge *BC* and then join the new vertex C' (note that in this situation $C' = B + 2BC$) to vertex *A* (see Fig. 8(b)): or the other equivalent, by carrying out an LE bisection of the original triangle and taking the acute sub-triangle generated (see Fig. 8(c)). These two possibilities will be taken into account in the discussion hereinafter.

Therefore, in order to obtain the different triangles t_{n1} generated by iterative application of the 7T-LE partition, we double the shortest edge *BC* successively, whenever the baseline *AB* is not the shortest edge of the triangle, until the last doubled edge becomes the longest

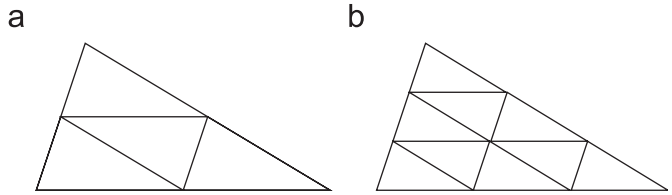

Fig. 14. Self-similar partitions depending on the number of points per edge. (a) one point per edge. (b) Two points per edge.

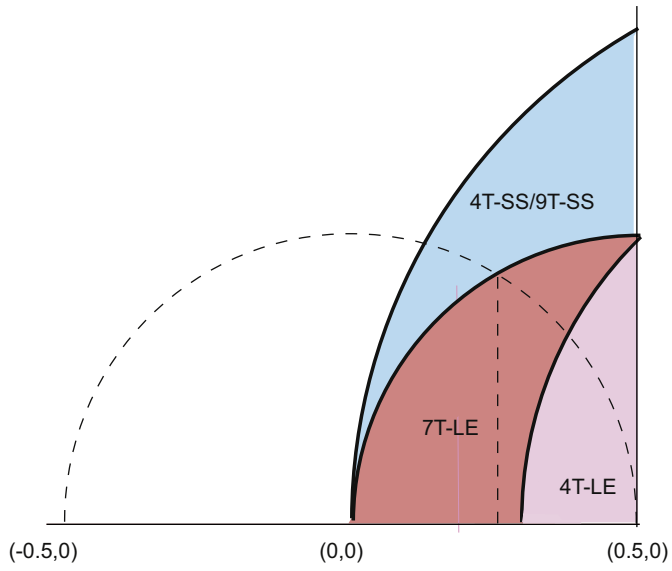

Fig. 15. Best partition for a triangle.

one of the new triangle generated. Supposing that the last doubled edge is *BC*, the new edge BC' is not the longest one, but *AB*, however, is the shortest one, that is $|AB| < |BC'| < |AC'|$, (see Fig. 9(a)).

Then, we double the edge *AB* and now, we can see how, in Fig. 9(b), AC' is the shortest edge. Therefore, if AB' is the longest edge, the last doubled edge becomes the longest one of the new triangle. If not, we can see that angle $\phi = \widehat{B'AC'} < \varphi = \widehat{ABC}$, that is, the new angle defined by the last doubled edge and the shortest one, is smaller than in the previous situation so, at some point, this process must end and the last doubled edge becomes the longest one.

Let us suppose, then, that, in our initial triangle $\Delta ABC \equiv t_0$, $|BC| < |AC| < |AB|$ and when we double *BC*, and new point $D = B + 2BC$ is generated, in triangle $\Delta ABD = t_{(i)}$, edge *BD* is the longest one, (see Figs. 10(a) and (b)). There are now two possibilities:

(1) If $|AD| > |AB|$, then the next new triangle produced by the 7T-LE partition, resulting from the LE bisection of triangle $t_{(i)}$, is triangle $t_0 = \Delta ABC$ which has been previously considered, and there the process ends.
(2) In the other case, i.e. if $|AD| < |AB| < |BD|$, then the next new triangle produced by the 7T-LE partition, resulting from the LE bisection of triangle $t_{(i)}$, is triangle $t_{(ii)} = \Delta ACD$. (See Fig. 10(c)). In this triangle, $|CD| = |BC| < |AC|$, so there are three cases to study:
   (a) First, if we presume that $|CD| < |AC| < |AD|$, then we double edge *CD* and we obtain triangle $t_{(i)}$ again.
   (b) Let us now presume that $|CD| < |AD| < |AC|$. Then we divide the longest edge *AC* and triangle $t_{(iii)} = \Delta CDE$ is obtained. See Fig. 10(d). It is easy to see that the shortest-edge of this new

Table 1
Sequences of dissimilar triangles obtained by the 4T-LE and 7T-LE partitions

It. n	4T-LE triangles no. of dissimilar triangles 15			7T-LE triangles no. of dissimilar triangles 7		
	γ_n	β_n	α_n	γ_n	β_n	α_n
Test 1: *Initial triangle* $t_0 = (145.455, 32.595, 1.950)$						
0	145.455	32.595	1.950	145.455	32.595	1.950
1	143.292	34.545	2.164	143.291	32.595	4.114
2	140.885	36.708	2.407	138.198	32.595	9.206
3	138.200	39.115	2.684	123.933	32.595	23.472
4	135.202	41.800	2.998	77.683	69.721	32.595
5	131.850	44.798	3.351	69.721	59.152	51.125
6	128.107	48.150	3.743	84.036	59.152	36.810
7	123.937	51.893	4.170	69.721	59.152	51.125
8	119.316	56.063	4.621			
9	114.235	60.684	5.081			
10	108.715	65.765	5.520			
11	102.811	71.285	5.904			
12	96.618	77.189	6.193			
13	90.266	83.382	6.352			
14	89.734	83.907	6.359			
15	90.266	83.382	6.352			
It. n	4T-LE Triangles no. of dissimilar triangles 11			7T-LE Triangles no. of dissimilar triangles 8		
	γ_n	β_n	α_n	γ_n	β_n	α_n
Test 2: *Initial triangle* $t_0 = (173.972, 5.423, 0.605)$						
0	173.972	5.423	0.605	173.972	5.423	0.605
1	173.216	6.028	0.756	173.215	5.423	1.361
2	172.245	6.784	0.971	170.949	5.423	3.627
3	170.952	7.755	1.293	153.689	20.887	5.4230
4	169.148	9.048	1.804	144.928	20.887	14.183
5	166.462	10.852	2.686	102.858	56.254	20.887
6	162.066	13.538	4.396	78.056	56.254	45.689
7	153.735	17.934	8.331	81.241	56.254	42.504
8	133.923	26.265	19.812	78.056	56.254	45.689
9	84.274	49.648	46.077			
10	95.726	43.599	40.676			
11	84.274	49.648	46.077			

Test problem 1 and test problem 2.

triangle is CE, so we double it, and we obtain triangle $t_{(ii)}$ again.

(c) Finally, we must consider $|AD| < |CD| < |AC|$. As in the previous case, we divide AC but, now, we obtain triangle $t_{(iv)} = \Delta ADE$. (See Fig. 10(d).) In this triangle, AE is the shortest-edge, so we double it and we obtain triangle $t_{(ii)}$ again. □

3.2. Comparison of the 4T-LE and 7T-LE partition for a random triangle

A geometric diagram is constructed as follows [20]: (1) for a given triangle or sub-triangle, the longest edge is scaled to have unit length. This forms the base of the diagram. (2) It follows that the set of all triangles is bounded by this horizontal segment (longest edge), defined by the points $(0, 0)$, $(1, 0)$, and by two bounding exterior circular arcs of unit-radius, centered, respectively, at $(1, 0)$ and at $(0, 0)$, as shown in Fig. 11.

Note also that, by reflection around the vertical line $x = \frac{1}{2}$, it is enough to consider the left half of the diagram, which is equivalent to positioning the smallest angle at point $(1, 0)$ and the second largest angle at point $(0, 0)$.

Our measurement of triangle quality, in this section, will be the smallest angle. For each random apex into the geometric diagram, we compare α_R, the smallest angle of the Rivara triangle with α_N, the smallest angle of the new triangle obtained in the 7T-LE partition. In this situation, there are regions where either α_R or α_N is better. These regions will be denoted, respectively, by R_R and R_N.

First of all we must study which of the angles in triangle t_{n_1} is the smallest. By applying the Law of Sines, we can see that

$$\alpha_N = \alpha_2 \quad \text{if } a^2 + b^2 < \left(\frac{1}{2}\right)^2 \text{ and } a < \frac{1}{4},$$

$$\alpha_N = \beta_2 \quad \text{if } \left(a - \frac{1}{2}\right)^2 + b^2 < \left(\frac{1}{2}\right)^2 \text{ and } a > \frac{1}{4} \text{ and}$$

$$\alpha_N = \gamma_2 \quad \text{in the rest of cases, that is, if } a^2 + b^2 > \left(\frac{1}{2}\right)^2 \text{ and } \left(a - \frac{1}{2}\right)^2 + b^2 > \left(\frac{1}{2}\right)^2.$$

These three possibilities correspond respectively to regions *II*, *III* and *I* in Fig. 12.

Now, we compare α_N with α_1, β_1 and γ_1. In region *I* we obtain that α_1 is always smaller than γ_2, so $\alpha_N > \alpha_R$. In region *II* we obtain that γ_1 is always smaller than α_2 so $\alpha_N > \alpha_R$ too. Finally, in region *III*, we find that β_2 is always smaller than β_1 and γ_1 and is smaller than α_1 when $(a-1)^2 + b^2 < \frac{1}{2}$, so, only in this case, $\alpha_N < \alpha_R$. In Fig. 13, we can see that regions R_R and R_N are separated by the circumference centered at $(1, 0)$ and with radius $1/\sqrt{2}$.

So if we compare the area covered by both regions, we obtain that the 7T-LE partition is better than the 4T-LE partition in 89% of the cases (more precisely, the areas of both regions are $A(R_R) = 0.07135$ and $A(R_N) = 0.6486$).

Finally, notice that similar partitions of acute triangles are better than longest-edge partitions. Fig. 14 shows similar partitions of an acute triangle, depending on the number of the points per edge.

In Fig. 15, we can see the rules which allow us to decide which of the various partitions to use. If $(a-1)^2 + b^2 < \frac{1}{2}$, we choose 4T-LE partition. If $(a-1)^2 + b^2 > \frac{1}{2}$ and $(a - \frac{1}{2})^2 + b^2 < (\frac{1}{2})^2$, we choose 7T-LE partition: and if $(a - \frac{1}{2})^2 + b^2 > (\frac{1}{2})^2$, we choose the self-similar partition.

Table 2
Sequences of dissimilar triangles obtained by the 4T-LE and 7T-LE partitions

It. n	4T-LE triangles—no. of dissimilar triangles 8			7T-LE triangles—no. of dissimilar triangles 7		
	γ_n	β_n	α_n	γ_n	β_n	α_n
Test 3: *Initial triangle* $t_0 = (169.900, 8.572, 1.527)$						
0	169.900	8.572	1.527	169.900	8.572	1.527
1	167.721	10.100	2.180	167.719	8.572	3.708
2	164.371	12.279	3.349	158.613	12.814	8.572
3	158.625	15.629	5.747	125.395	41.790	12.814
4	146.921	21.375	11.704	106.818	41.790	31.391
5	117.268	33.079	29.652	75.424	62.784	41.790
6	63.237	62.732	54.031	73.181	62.784	44.033
7	116.763	33.270	29.967	75.424	62.784	41.790
8	63.237	62.732	54.031			
It. n	4T-LE triangles—no. of dissimilar triangles 4			7T-LE triangles–no. of dissimilar triangles 4		
	γ_n	β_n	α_n	γ_n	β_n	α_n
Test 4: *Initial triangle* $t_0 = (114.624, 54.900, 10.475)$						
0	114.624	54.900	10.475	114.624	54.900	10.475
1	102.073	65.376	12.551	102.074	54.900	23.254
2	88.250	77.927	13.824	74.624	54.900	50.475
3	91.750	74.623	13.627	86.500	54.900	38.598
4	88.250	77.927	13.824	74.624	54.900	50.475
5						
6						

Test problem 3 and test problem 4.

It should be noted that for a complete specification of local refinement based on the 7T-LE partition, there is a need to define how to achieve the conformity of the mesh. This will be tackled in a forthcoming paper [21].

4. Numerical examples

In this section, we present two different experiments. First, some test triangles also studied by Rivara and Iribarren in [19] and Plaza *et al.* in [18], were chosen to compare the evolution of the triangles generated by the 4T-LE partition with the new triangles generated by the 7T-LE partition. Second, we draw a comparison between the 7T-LE partition and the 7T-Delaunay partition.

4.1. The 7T-LE versus 4T-LE for mesh quality improvement

Although we have already underlined the different behaviour with respect to mesh quality improvement given by the 7T-LE partition and the 4T-LE partition, here we present some numerical examples for different initial triangles t_0. Tables 1 and 2 show four test problems in which the sequence of dissimilar triangles are obtained by the 4T-LE and by the 7T-LE partition. Note that the new triangles generated by the 7T-LE partition are better shaped than the corresponding triangles generated by the 4T-LE partition. However, in test problems 2 and 3, the last (acute) triangles generated by the 4T-LE partition are better (in terms of the minimum angle) than the last new triangles generated by the 7T-LE. For a visual comparison of the evolution of the triangles, see Fig. 18.

In order to visually compare the better improvement achieved by means of the 7T-LE partition, see Fig. 16, in which, and for example test 1, the evolution of the smallest and largest angles for each of the new triangles generated by the 7T-LE partition is shown. The initial triangle is $t_0 = (\alpha, \beta, \gamma) = (1.95, 32.595, 145.455)$ as in Rivara and Iribarren [19]. Compare the evolution of these angles with the evolution of the triangles generated by the 4T-LE partition given in Fig. 4 at page 7.

For a better understanding of the self-improvement property of the 4T-LE partition, and the limits of this property as given in this paper, the successive triangles obtained have been normalized

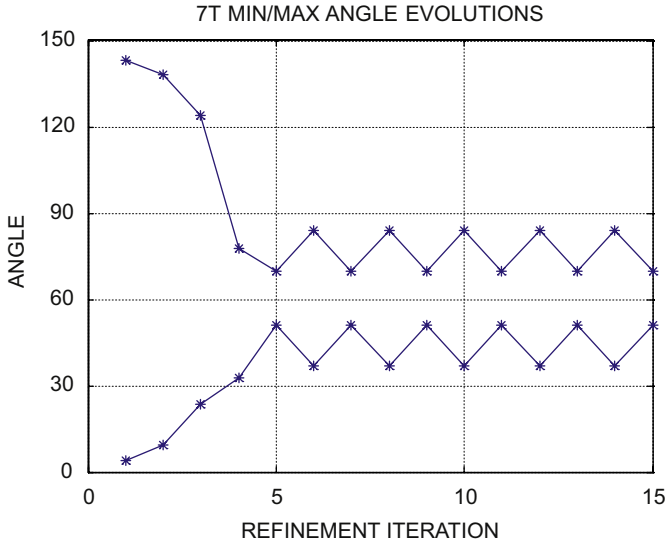

Fig. 16. Evolution of minimum and maximum angles of the new triangles generated by the 7T-LE partition, one at a time, for example test 1: $t_0 = (145.455, 32.595, 1.950)$.

to share the longest edge. Fig. 17 shows the triangles obtained by the 4T-LE and by the 7T-LE partition in the first test problem. Since all the triangles have been represented with longest edge on vertices $(0, 0)$ and $(0, 1)$, the evolution of the new triangles generated by the 7T-LE partition vs. the triangles generated by the 4T-LE partition can be observed, at a glance, from the diagrams in Fig. 18, where the third vertices are joined by lines, from bottom to top.

It should be noted that, in the case of the last triangles generated by the 7T-LE partition in these tests, it would seem that the largest of the smallest angles generated does not depend upon the geometry of the initial triangle considered. This contrasts sharply with the situation for the 4T-LE partition, in which these angles improve, but within certain limits, depending upon the values of the angles of the initial triangle.

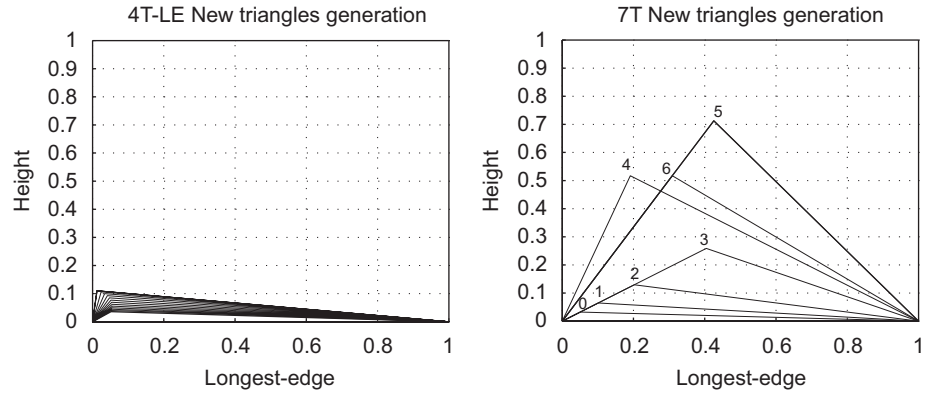

Fig. 17. Evolution of dissimilar triangles of example test 1.

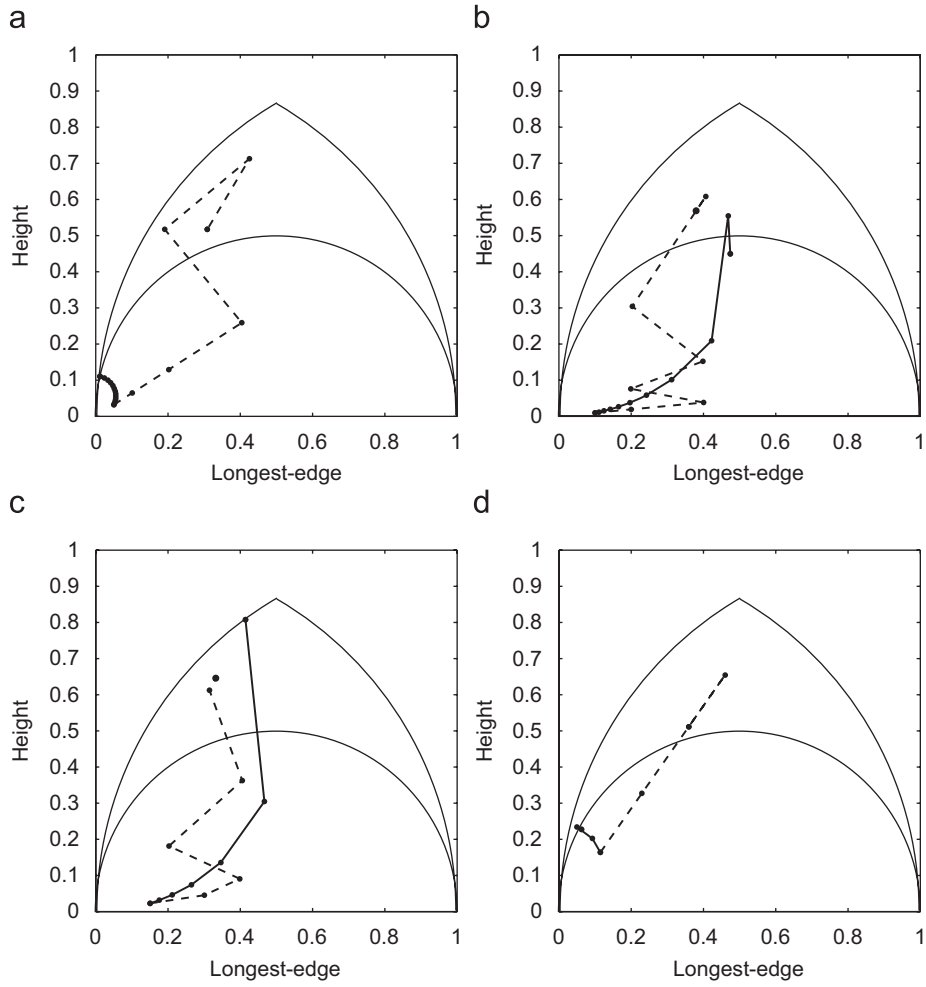

Fig. 18. Evolution of the triangles given by the 4T-LE partition (solid line) vs. 7T-LE partition (dashed line). (a) Example test 1. (b) Example test 2. (c) Example test 3. (d) Example test 4.

In order to experimentally check this conjecture, we carried out the following computational experiment. Select a point (x, y) within the mapping domain comprised the horizontal segment of extreme points $(0, 0)$ and $(1, 0)$, and the unit circular arcs which centre at these extreme points. Point (x, y) defines the apex of a target triangle with additional vertices at $(0, 0)$ and $(1, 0)$. For this triangle, 7T-LE division is successively applied as long as a new dissimilar t_{n1} triangle appears. This means that we recursively apply 7T-LE and stop when the shapes of new generated triangles are the same as those already generated in previous refinement step. The number of such refinements to reach termination defines the number of dissimilar triangles associated with the initial triangle, and this numerical value is assigned to the initial point (x, y) chosen. This process is progressively applied to a large sample of triangles

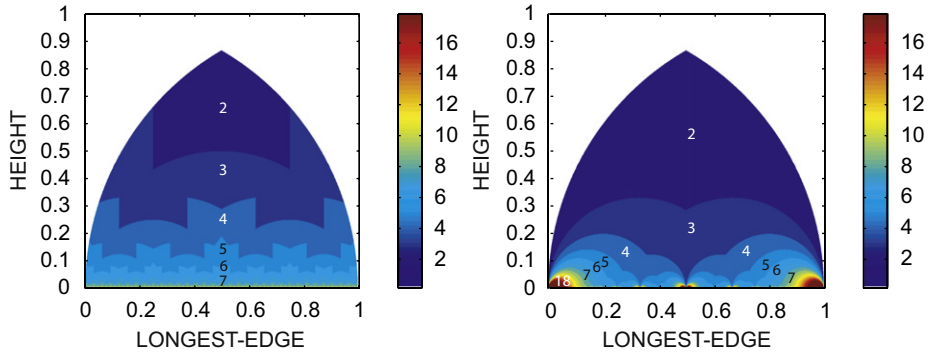

Fig. 19. Dissimilar triangle classes generated by computer experiment for the 7T-LE (a) vs. 4T-LE partition (b).

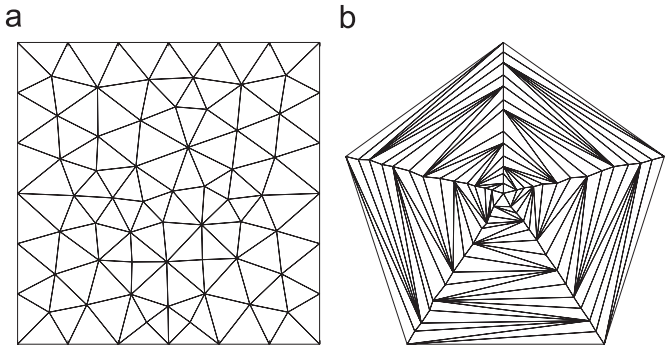

Fig. 20. Two different initial triangulations. (a) Good quality mesh. (b) Bad quality mesh.

(points) uniformly distributed over the domain. Finally, we graph the respective values of dissimilar triangles in a corresponding colour map to obtain the result in Fig. 19(a). The same experiment for the 4T-LE partition is shown in Fig. 19(b).

It should be noted that the dark blue region in Fig. 19 corresponds to the region in which all the trajectories end, with total independence of the initial position. Therefore, for the 7T-LE partition, a lower bound for the maximum of the smallest angles for triangles t_{n1} is $\alpha = 30°$ corresponding to the apex with $x = \frac{1}{4}$, or the apex with $x = \frac{3}{4}$. Note also that the smallest angle in each of the regions generated in this way, is bounded from below with total independence of the initial point of the respective trajectories. This is a remarkable feature in comparison with the evolution of the angles for the 4T-LE partition. In the 4T-LE partition, these lower bounds depend on the geometry of the initial triangle. See [18] for details on the evolution of the angles when the 4T-LE partition is recursively applied. Also observe the evolution of the minimum angles in Tables 1 and 2.

4.2. A comparative study of two seven-triangle partitions

Here we show a numerical comparison of the seven-triangle partitions previously presented. Namely, we apply these partitions to an initial (good quality) Delaunay mesh, and to a (poor quality) initial pentagonal mesh. See Fig. 20.

For a comparison of the quality measurement evolution when each partition is globally applied, the mean value of the quality measurement η has been calculated. Bearing in mind that for each triangle t, the quality measurement η is defined by

$$\eta(t) = \frac{4A\sqrt{3}}{l_1^2 + l_2^2 + l_3^2}$$

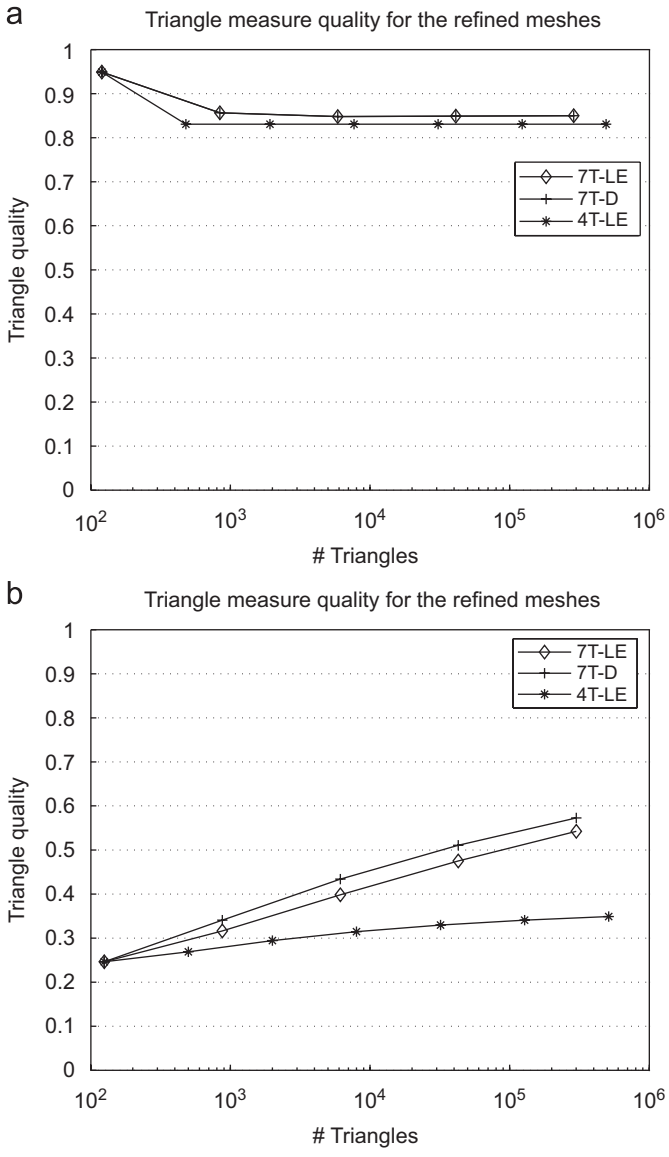

Fig. 21. Evolution of mesh quality. (a) Good quality mesh. (b) Bad quality mesh.

where A is the area of t, and l_1, l_2 and l_3 the lengths of the sides of the triangle. If $\eta(t) > 0.6$, triangle t is acceptable quality-wise. For the equilateral triangle $\eta = 1$ where $l_1 = l_2 = l_3 = \sqrt{\frac{4A\sqrt{3}}{3}}$, see [4]. It

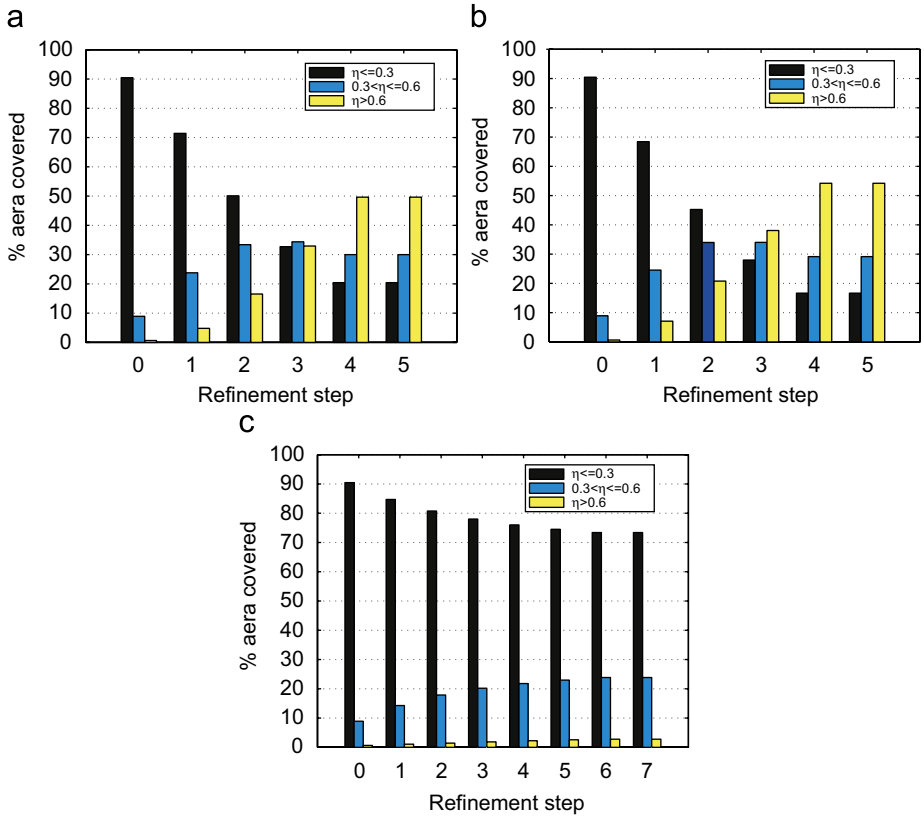

Fig. 22. Distribution of triangles (percentages) for different triangle partitions from a poor quality mesh. (a) 7T-LE partition. (b) 7T-Delaunay partition. (c) 4T-LE partition.

should also be noted that other quality measurements may be used for this purpose, but they give similar patterns [22,23].

Fig. 21 shows the evolution of the average of $\eta(t)$ for the triangles t, at each mesh level, when the three reference partitions, 4T-LE, 7T-LE and 7T-Delaunay, are repeatedly applied to every triangle, and successive generations, for the two different initial meshes considered here. Note that the 7T-LE partition is equivalent to the 7T-Delaunay in the case of an initially good-quality mesh, whereas the evolution is a little worse than that of the 7T-Delaunay when the initial mesh is relatively poor quality. However, in both cases, the quality evolution demonstrated by the 7T-LE partition is much better than that given with the 4T-LE partition. The clear advantage of the 7T-LE partition in comparison with the 4T-LE partition is more evident if the percentage of area covered by different classes of triangles is considered. To this end, we have classified the triangles as follows:

- Class A: triangles with $0.6 < \eta \leqslant 1$.
- Class B: triangles with $0.3 < \eta \leqslant 0.6$.
- Class C: triangles with $0 < \eta \leqslant 0.3$.

The evolution of the corresponding percentage of area covered by these three classes of triangles, in the case of an initial bad quality mesh (pentagonal mesh) is given in Fig. 22. For this initial bad quality mesh, the results given are really spectacular, since the percentage of bad elements decreases monotonously when the refinement level increases. In addition, the 7T-LE partition behaves similarly to the 7T-Delaunay partition, and much better than the 4T-LE partition.

But the 7T-LE not only shows better behaviour considering the average of the quality measurement, but also when the distribution of the quality of the measurement values is considered. This is underlined in Fig. 22 for the finest mesh obtained from an initial bad quality mesh, respectively, by the 7T-LE partition and the 4T-LE partition.

It should be pointed out here that, from a computational point of view, the 7T-LE partition is cheaper than the 7T-Delaunay partition since the 7T-LE partition is linear to the number of points $O(N)$, while the 7T-LE is $O(N \lg N)$ [10], and, hence, it will be advantageous in many scenarios.

5. Conclusions

In this paper, the seven-triangle longest-edge (7T-LE) partition has been presented and studied. It has been proved that the iterative application of the 7T-LE partition to any initial triangle generates a finite number of dissimilar triangles. The so-called self-improvement property of this partition has been studied and compared with the same property of the four-triangle longest-edge partition of Rivara. The triangles generated by iterative application of the 7T-LE partition tend to be improved throughout the process, in the sense that the percentage of area covered by bad elements tends to decrease, while the percentage of good elements tends to increase when the number of global refinements increases, which is especially true in the case of bad initial triangles. It should also be highlighted that a lower bound for the maximum of the smallest angles of the new triangles t_{n1} generated by the 7T-LE partition is $\alpha = 30^\circ$, and this bound is independent of the geometry of the initial triangle.

Acknowledgement

This work has been supported in part by CICYT Project number MTM2005-08441-C02-02 from Ministerio de Educación y Ciencia of Spain.

References

[1] G.F. Carey, Computational Grids: Generation, Refinement and Solution Strategies, Taylor & Francis, London, 1997.

[2] D.N. Arnold, A. Mukherjee, L. Pouly, Locally adapted tetrahedral meshes using bisection, SIAM J. Sci. Comput. 22 (2) (2000) 431–448.

[3] E. Bänch, Local mesh refinement in 2 and 3 dimensions, IMPACT Comput. Sci. Eng. 3 (1991) 181–191.

[4] E. Bank, PLTMG: a software package for solving elliptic partial differential equations, Users' Guide 9.0, Department of Mathematics, University of California at San Diego, 2004.

[5] S.W. Bova, G.F. Carey, Mesh generation/refinement using fractal concepts and iterated function systems, Int. J. Numer. Methods Eng. 33 (1992) 287–305.

[6] J.M. Maubach, Local bisection refinement for *n*-simplicial grids generated by reflection, SIAM J. Sci. Stat. Comput. 16 (1) (1995) 210–227.

[7] M.A. Padrón, J.P. Suárez, A. Plaza, Refinement based on longest-edge and self-similar four-triangle partitions, Math. Comput. Simulation 75 (5–6) (2007) 251–262.

[8] S. Kumar, Robust incremental polygon triangulation for fast surface rendering, J. WSCG 8 (1) (2000).

[9] M. Bern, D. Eppstein, Mesh generation and optimal triangulation, in: D.-Z. Du, F.K. Hwang (Eds.), Computing in Euclidean Geometry, second ed., World Scientific, Singapore, 1995, pp. 47–123.

[10] G.V.V. Rabi Kumar, P. Srinivasan, K.G. Shastry, B.G. Prakash, Geometry based triangulation of multiple trimmed NURBS surfaces, Comput. Aided Des. 33 (2001) 439–454.

[11] N. Hitschfeld, L. Villablanca, J. Krause, M.-C. Rivara, Improving the quality of meshes for the simulation of semiconductor devices using Lepp-based algorithms, Int. J. Numer. Methods Eng. 58 (2003) 333–347.

[12] M.-C. Rivara, N. Hitschfeld, B. Simpson, Terminal-edges Delaunay (small-angle based) algorithm for the quality triangulation problem, Comput. Aided Des. 33 (2001) 263–273.

[13] A.P. DelaHoz, The fractal behaviour of triangular refined/derefined meshes, Commun. Numer. Methods Eng. 12 (5) (1996) 295–302.

[14] A. Plaza, J.P. Suárez, M.A. Padrón, Fractality of refined triangular grids and space-filling curves, Eng. Comput. 20 (4) (2005) 323–332.

[15] W.F. Mitchell, Optimal multilevel iterative methods for adaptive grids, SIAM J. Sci. Stat. Comput. 13 (1992) 146–167.

[16] M.-C. Rivara, Algorithms for refining triangular grids suitable for adaptive and multigrid techniques, Inter. J. Numer. Methods Eng. 20 (1984) 745–756.

[17] I. Rosenberg, F. Stenger, A lower bound on the angles of triangles constructed by bisecting the longest side, Math. Comput. 29 (1975) 390–395.

[18] A. Plaza, J.P. Suárez, M.A. Padrón, S. Falcón, D. Amieiro, Mesh quality improvement and other properties in the four-triangles longest-edge partition, Comput. Aided Geometric Des. 21 (4) (2004) 353–369.

[19] M.-C. Rivara, G. Iribarren, The 4-triangles longest-side partition of triangles and linear refinement algorithms, Math. Comput. 65 (216) (1996) 1485–1502.

[20] A. Plaza, J.P. Suárez, G.F. Carey, A geometric diagram and hybrid scheme for triangle subdivision, Comput. Aided Geometric Des. 24 (1) (2007) 19–27.

[21] A. Plaza, A. Márquez, A. Moreno-González, J.P. Suárez, Local refinement based on the 7-triangle longest-edge partition, Math. Comput. Simulation 2008, to appear.

[22] V.N. Parthasarathy, C.M. Graichen, A.F. Hathaway, A comparison of tetrahedron quality meshes, Finite Elem. Anal. Des. 15 (3) (1994) 255–261.

[23] A. Plaza, M.A. Padrón, J.P. Suárez, Non-degeneracy study of the 8-tetrahedra longest-edge partition, Appl. Numer. Math. 55 (4) (2005) 458–472.